




Co-delivery of artemisinin and metformin via PEGylated niosomal nanoparticles: potential anti-cancer effect in treatment of lung cancer cells

Salah Jaafar Abdulkareem¹ · Davoud Jafari-Gharabaghlo¹ · Mahdi Farhoudi-Sefidan-Jadid¹ · Elnaz Salmani-Javan¹ · Fatemeh Toroghi² · Nosratollah Zarghami^{1,3} 

Received: 4 March 2023 / Accepted: 5 December 2023 / Published online: 3 January 2024
© The Author(s), under exclusive licence to Tehran University of Medical Sciences 2024

Abstract

Purpose Despite the advances in treatment, lung cancer is a global concern and necessitates the development of new treatments. Biguanides like metformin (MET) and artemisinin (ART) have recently been discovered to have anti-cancer properties. As a consequence, in the current study, the anti-cancer effect of MET and ART co-encapsulated in niosomal nanoparticles on lung cancer cells was examined to establish an innovative therapy technique.

Methods Niosomal nanoparticles (Nio-NPs) were synthesized by thin-film hydration method, and their physicochemical properties were assessed by FTIR. The morphology of Nio-NPs was evaluated with FE-SEM and AFM. The MTT assay was applied to evaluate the cytotoxic effects of free MET, free ART, their encapsulated form with Nio-NPs, as well as their combination, on A549 cells. Apoptosis assay was utilized to detect the biological processes involved with programmed cell death. The arrest of cell cycle in response to drugs was assessed using a cell cycle assay. Following a 48-h drug treatment, the expression level of hTERT, Cyclin D1, BAX, BCL-2, Caspase 3, and 7 genes were assessed using the qRT-PCR method.

Results Both MET and ART reduced the survival rate of lung cancer cells in the dose-dependent manner. The IC₅₀ values of pure ART and MET were 195.2 μM and 14.6 mM, respectively while in nano formulated form their IC₅₀ values decreased to 56.7 μM and 78.3 μM, respectively. The combination of MET and ART synergistically decreased the proliferation of lung cancer cells, compared to the single treatments. Importantly, the combination of MET and ART had a higher anti-proliferative impact against A549 lung cancer cells, with lower IC₅₀ values. According to the result of Real-time PCR, hTERT, Cyclin D1, BAX, BCL-2, Caspase 3, and Caspase 7 genes expression were considerably altered in treated with combination of nano formulated MET and ART compared to single therapies.

Conclusion The results of this study showed that the combination of MET and ART encapsulated in Nio-NPs could be useful for the treatment of lung cancer and can increase the efficiency of lung cancer treatment.

Keywords Metformin · Artemisinin · Lung cancer · Niosome · Combination therapy

Salah Jaafar Abdulkareem and Davoud Jafari-Gharabaghlo are co-first authors and contributed equally to this work

✉ Nosratollah Zarghami
zarghamin@gmail.com

¹ Department of Clinical Biochemistry and Laboratory Medicine, Faculty of Medicine, Tabriz University of Medical Sciences, Tabriz, Iran

² Research Center for Molecular Medicine, Hamedan University of Medical Science, Hamedan, Iran

³ Department of Medical Biochemistry, Faculty of Medicine, Istanbul Aydin University, Istanbul, Turkey

Introduction

Lung cancer is one of the most frequently reported malignancies in the world population which has been known as the leading reason for cancer-related inevitable death in the past few decades. For instance, in 2018, 2,093,876 new cases of lung cancer were reported in the world and 1,761,007 people died due to lung cancer [1]. Tobacco consumption has emerged as one of the main reasons of lung cancer which accounts for 82% of all deaths in 2021. Furthermore, non-smoker-related lung cancer is one of the top ten motives of cancer fatalities in both sexes and among them, men have a smaller portion of nonsmoking-related lung cancer than

women [2]. Based on histopathological characteristics, lung cancer is divided into two primary categories: non-small-cell lung cancer (NSCLC) and small-cell lung cancer (SCLC), responsible for 85 and 15 percent of cases respectively [3]. Understanding lung cancer classification and its biological characterizations are important for lung cancer therapy. For instance, SCLCs, which are invasive subtypes, are treated non-surgically while NSCLCs are treated by a combination of surgery and adjuvant therapy [4]. Lung cancer is treated and cured using surgery, radiation, chemotherapy targeted therapies, and immunotherapy whether alone or in combination but these agents cause several side effects and are ineffective in some cases [5–8] thus new treatment should be developed.

For centuries, plants have been used to treat various diseases, which in most cases had minimal side effects. Perceiving the increasing tendency of human societies to use natural treatments including herbal therapy, trying to identify effective herbal compounds, and providing new methods for targeted therapy is considered a necessity [9]. The results of *in vitro* research have shown that various compounds such as curcumin, metformin, and silybin can have a suppressive effect on the growth and metastasis of cancer cells. Now, more experiments are designed to understand their molecular mechanisms [10, 11].

Sometimes repurposing old drugs that are used to remedy non-cancerous diseases can speed up the process of introducing potential anti-cancer drugs. Previously, the ability of metformin and artemisinin to inhibit various types of cancer has been investigated. Although these studies concluded more investigation is needed, the results were generally promising [12].

Metformin (MET) as a kind of biguanide is the most commonly prescribed drug in type II diabetes [13, 14]. It is proven that MET has anticancer effects on several types of cancers such as gastric carcinoma, pancreatic cancer, medullary thyroid, and uterine cancer because this drug can suppress cancer cell development, trigger apoptosis, and cell cycle arrest [14–18]. Also based on a recent study, MET had a remarkable effect on lung cancer. Patients who received MET, had lower risk and their survival rate for lung cancer increased. In addition, MET has a protective effect on SCLC and NSCLC patients [19, 20]. MET anti-cancer effect is through inhibition of phosphoinositide 3-kinase/Akt/ mTOR signaling pathways and activation of AMPK [21, 22].

Artemisinin (ART) is a Chinese herbal medicine that has been approved against the plasmodium parasite [23] and has recently been reported to be an effective drug for COVID-19 [24]. Recent studies have shown that ART could be the best tool to prevent cancer cells development and proliferation, inhibit angiogenesis, cell cycle arrest, and interrupt cell migration, which can selectively destroy cancerous cells [23, 25, 26]. According to recent data, ART induces

ROS-dependent apoptosis/ferroptosis and consequently suppresses the proliferation of lung cancer cells [27]. ART has no significant cytotoxic effect on normal cells compared to chemotherapy [25].

Combination therapy is a therapy that uses several therapeutic agents simultaneously and is known as a foundation stone of cancer treatment. Combination therapy compared with monotherapy, significantly reduces drug resistance, tumor growth, and cancer stem cells development as well as apoptosis induction. Since multiple signaling pathways are targeted in combination therapy, fewer therapeutic agents are needed and toxicity is reduced [22, 28–31].

Human telomerase reverse transcriptase (hTERT), is the catalytic subunit of telomerase enzyme which is responsible for the replication of chromosomal telomeres during cell division [32]. Several studies have shown that maintenance of telomerase length is a feature of tumor cells and overexpression of hTERT and increased telomerase length has been found in various malignancies including lung cancer, and for these reasons, inhibition of hTERT is an attractive target for cancer therapy and also has provided an opportunity for lung cancer treatment [33–36].

BAX/BAK are pro-apoptotic molecules that induce cell death during the apoptosis process. The BCL-2 family of proteins is involved in the suppression of BAX/BAK. BCL-2 overexpression has been linked to a variety of malignancies, making BCL-2 a promising anti-cancer therapy [37, 38]. Caspases are a kind of cysteine protease that plays an important part in apoptosis and is activated in response to cell death signals. Caspases 3 and 7 are the major executioner caspases among the caspases [39–41]. Many specific proteins, such as Cyclin-dependent kinases (CDKs), regulate the transition phases of the cell cycle [42]. CDKs are normally inactive and are activated when cyclins bind to them [43, 44]. For instance, cyclin D, which includes cyclin D1, cyclin D2, and cyclin D3. Cyclin D synthesis begins during G1 and causes the G1/S phase transition [45]. Cyclins and CDKs blockers have recently been reported to be helpful in preventing tumor cell proliferation, inducing an aging-like phenotype, and affecting cellular metabolism [46, 47]. Thus, developing effective therapeutic agents should be a priority.

In the treatment of cancer, nano-sized carriers have gained attention due to reducing drug's side effects and improving the effectiveness of drugs [48]. Different types of nanocarriers including liposomes, polymers, niosomes, and micelles are available. Niosomes (Non-Ionic Surfactant Vesicles) are biocompatible and biodegradable nanoparticles which used to deliver drugs through ocular delivery, pulmonary, transdermal, oral, and across the blood–brain barrier [49–52]. Furthermore, niosomes can entrap and deliver both lipophilic and hydrophilic drugs [49]. These features are also seen in liposomes. However, compared to liposomes, niosomes have advantages: they are less

expensive to produce, easier to formulate, and much more stable. Niosomes owe this stability to the presence of non-ionic surfactants in their structure, which are physically and chemically more stable than lipids [53].

Based on recent studies, MET, and ART demonstrated anticancer effects on lung cancer cells, and the combination of both may be more effective in lung cancer suppression. In this study, we examined the effect of MET, ART, ART-MET in the free and encapsulated form on lung cancer cell proliferation and the expression level of hTERT, Cyclin D1, BAX, BCL-2, Caspase 3, and 7.

Materials and methods

1- NPs preparation

The thin-film hydration method was used to prepare blank Nio-NPs in several steps. Briefly, a mixture of PEG (3 mg), span 60 (36.6 mg), and cholesterol (5.7 mg) were dissolved in a combination of methanol (6 ml) and Chloroform (3 ml). A rotary evaporator was used to remove solvents from the solution (55–65 °C for 1 h at 0.46 atm). The resulting mixture was cooled (23 °C) then PBS (10 ml) was added and the solution was reconnected to the rotary evaporator (1 h, 55–65 °C, 0.09 atm). Finally, an ultrasonicator was used to mix the solution (24 °C for 30 min) and for future usage, the final solution was kept at 4 °C. To fabricate MET loaded niosomal NPs (MNP), the same steps and amounts were used with 1.6 mg of MET which was dissolved in the hydration step (second step) in PBS. To fabricate ART loaded niosomal NPs (ANP), 2.8 mg of ART was dissolved in methanol and Chloroform along with other materials with the previously mentioned amounts and steps. Finally, to fabricate ART-MET loaded niosomal NPs (ANP-MNP), 3 mg of PEG, 36.6 mg of Span 60, 5.7 mg of Cholesterol, and 2.8 mg of ART dissolved in methanol (6 ml) and Chloroform (3 ml) mixture with same steps and conditions, except in hydration step 1.6 mg of MET was also dissolved in PBS.

2- NPs characterization

After diluting the NPs in PBS with a ratio of 1 to 10, a Dynamic Light Scattering (DLS) technique (Nano ZS, Malvern Instruments Ltd., Malvern, UK) was employed at 25 °C, to evaluate the mean size, polydispersity index (PDI), and surface charge zeta potential of NPs [54, 55]. The samples were freeze-dried by a freeze-dryer (Dena Vacuum, FD-5005-BT, Iran). The morphology of NPs was evaluated utilizing a field emission scanning electron microscope (FE-SEM) (Hitachi S-4800, Japan) operating at an accelerating voltage of 15 kV. Prior to imaging, the samples were coated with a thin layer of gold through sputter-coating and an

atomic force microscope (AFM) (JPK Instruments AG, Berlin, Germany) which used freeze-dried form of NPs [54, 55]. Fourier-transform infrared spectroscopy (FTIR) (Shimadzu 8400 S, Kyoto, Japan) was used to get Physio-Chemical structure information of NPs. The FTIR analyses were conducted at room temperature across a scanning range of 4000 to 400 cm⁻¹ with a constant resolution of 4 cm⁻¹ [54, 56].

3- Drug encapsulation efficiency

The encapsulation efficiency was assessed using an ultrafiltration technique. In this method, 1 mL of the Nio-NPs formulation were placed in the inner compartment of Ultracel-30K Millipore filters, which have a molecular weight cutoff (MWCO) of 30,000 Da (Millipore Corporation, Billerica, MA). The filters were centrifuged at 4000g for 20 min at 4 °C (Eppendorf®, Hamburg, Germany). During the centrifugation process, the drugs loaded in the niosomes remained in the inner compartment, while free drugs passed through the filter membrane into the outer compartment. The quantity of free drugs was determined at 258 nm (for ART) and 234 nm (for MET) using a Shimadzu UV 2550 spectrophotometer. Then the following formulae were used to compute the percentage of entrapped medicines (encapsulation efficiency) and drug loading:

$$\text{Encapsulation efficiency} = \frac{\text{Weight of ART or MET in niosome}}{\text{Weight of initial ART or MET}} \times 100\%$$

4- Drug release study

To assess the release of ART and MET from NPs, a dialysis method was used. In brief, 30 mg of ANP and 30 mg of MNP loaded niosomal NPs were diffused in 5 mL of PBS (pH 7.4 and pH 5) and then transferred to a dialysis tube, swirled at 130 rpm. An equivalent amount of fresh PBS solution was added to the environmental buffer solution at regular intervals. Then the amount of the released ART and MET in the removed PBS was determined using a Shimadzu UV 2550 spectrophotometer at the wavelengths 258 nm (ART) and 234 nm (MET) [56, 57].

5- Cell culture

The Pasteur Institute of Iran's cell bank provided the A549 lung cancer cell line which was cultured in RPMI 1640 (Gibco, USA) enriched with 10% FBS (Biocrom, UK), and penicillin/streptomycin (1%, Sigma, Germany). The cells were maintained at 37 °C in a humidified environment with 5% CO₂ [56, 58].

6- Cytotoxicity assay

For evaluation cytotoxic effects of ART, MET, and their nano encapsulated form on A549 cell line MTT assay was performed. Briefly, A549 cells were seeded in a 96-well plate (1×10^6 cells/well) and allowed to attach at 37 °C with 5% CO₂. After 24 h, cells were exposure for 48 h with various dosages of ART (0, 100, 200, 300, and 400 μM), MET (0, 5, 10, 15, 30, and 40 mM), ANP (0, 100, 200, 300, and 400 μM), MNP (0, 5, 10, 15, 30, and 40 mM), and their combination. The wells were emptied and filled with 200 μL of MTT (Sigma, Germany) and incubated for 4 h afterward wells were emptied again and 200 μL of DMSO (Merck, Germany) was added to each well and was shaken for 10 min [54, 59]. The IC₅₀ was calculated using Graph Pad 8.4 software after measuring the optical density at 570 nm in a microplate reader.

7- Real-time PCR

The qRT-PCR method was applied to determine the expression levels of studied genes. A549 cells were seeded in a 6-well plate (2×10^6 cells/well) and incubated for 24 h at 37 °C with 5% CO₂. Following that, cells were cultured for 48 h with IC₅₀ doses of ART, MET, ANP, MNP, and their combination. Total RNA was obtained using the Trizol (Sigma, Germany) reagent, reverse transcription was accomplished and cDNA was produced using the cDNA synthesis kit, all based on the manufacturer's instructions. The expression level of hTERT, Cyclin D1, BAX, BCL-2, caspase 3, and 7 genes were measured [56, 60].

8- Apoptosis analysis

A flow cytometer and Annexin V-FITC staining method were used to detect induction of early and late apoptosis. In brief, 2×10^5 cancer cells were seeded in each well of a 6-well plate and after 24 h treated with drugs for 48 h. Then the cells were then trypsinized and washed with PBS solution, then cells were re-suspended in 500 μL of binding buffer. Following the producer's guidelines, 5 μL of Annexin V reagent was applied, and cells were stained for 10 min. The cells mortality rate was evaluated using a flow cytometer after 1 μL of PI was introduced and incubated for 5 min [58, 59, 61].

10- Cell cycle analysis

2×10^6 A549 cells were seeded into each well of 6-well plates and left to attach overnight. For 48 h, cells were treated with ART, MET, ANP, MNP, and their combination at respective IC₅₀ concentrations. Following incubation, the cells were trypsinized, washed, and fixed with 1 ml of 70%

ethanol and stored overnight at -20 °C. For 30 min at 37 °C, the cells were collected and resuspended in PBS containing RNase (25 g/ml) and propidium iodide (PI, 50 g/ml). A flow cytometry was used to examine stained cells [59].

Results and discussion

Characterization of niosomal NPs

Usually, the place of drug administration is different from the place of its therapeutic effect. This issue is the basis of research on drug delivery systems, among which NPs are of great importance [62]. NPs could increase the half-life of drugs, maintain the stability of hydrophobic drugs in aqueous conditions, and control the drug release at the target site [63]. NPs size varies from 100 to 500 nm, they can pass through the blood–brain barrier, and the pulmonary system or be absorbed via the skin's tight junctions [64]. In this study, PEGylated-niosomal NPs were used to deliver of MET and ART to lung cancer cells. Niosomes are vesicular nanocarriers that have been extensively studied for drug delivery applications. They are composed of a bilayer hydrophobic membrane enclosing a central cavity filled with an aqueous phase, allowing them to encapsulate and deliver both hydrophobic and hydrophilic substances [65]. This characteristic makes niosomes suitable for loading a wide range of drugs, including hydrophobic (ART) and hydrophilic (MET) solubilities. The size, polydispersity index (PDI), and zeta potential of nanoparticles have significant effects on their characteristics and behavior. Size refers to the dimensions of nanoparticles and is an important parameter that affects their stability, drug loading capacity, and cellular uptake. The size of niosomes is also an important parameter that can affect their stability, drug loading capacity, and release kinetics [66]. Smaller nanoparticles generally have a larger surface area, which can enhance drug loading and improve cellular uptake [67]. Polydispersity index (PDI) is a measure of the size distribution of particles in a sample. A lower PDI value indicates a more uniform size distribution, while a higher PDI value suggests the presence of aggregates or a broader size range [68]. Zeta potential is an important parameter in the characterization of niosomes, as it provides information about the surface charge and stability of the particles. The zeta potential value indicates the degree of repulsion between particles, with higher absolute values indicating greater stability and lower likelihood of aggregation [69]. A zeta potential near ± 30 mV is generally considered to guarantee long-term stability of the formulation [69].

According to the DLS analysis results the mean diameter of synthesized blank Nio-NPs, ANP, MNP, and ANP-MNP in this study were 163 ± 3.94 , 183 ± 6.47 , 179 ± 5.13 ,

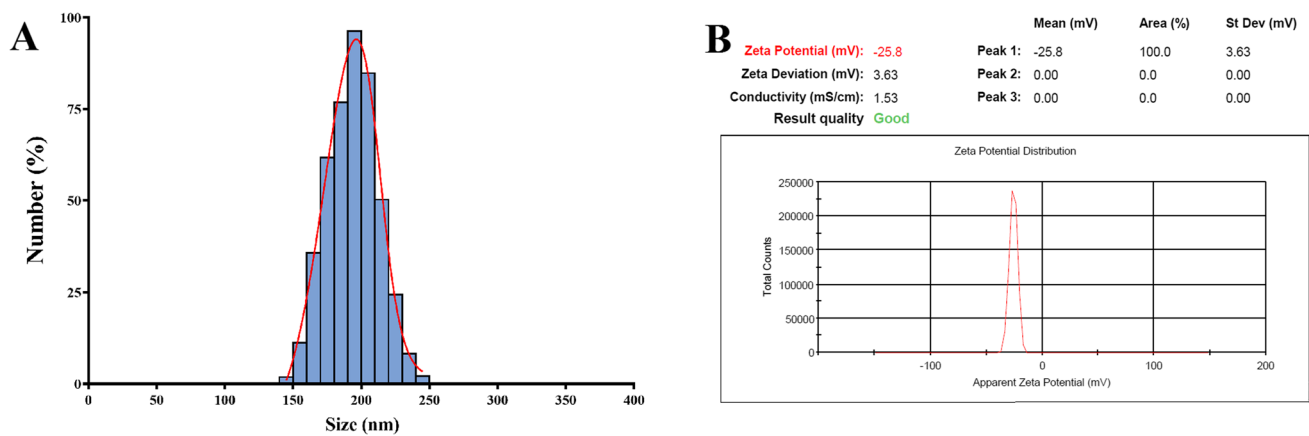


Fig. 1 Characterization of ART-MET loaded Nio-NPs size, PDI (A), and zeta potential (B). DLS method was used for analyses of size, PDI, and zeta potential of ART-MET loaded Nio-NPs

Table 1 DLS analyses of blank Nio-NPs, ANP, and MNP

Groups	Size (nm)	Polydispersity Index (PDI)	Zeta potential (mV)
Blank Niosome	163 ± 3.94	0.741	-19.4 ± 2.86
Metf-loaded Niosome	179 ± 5.13	0.863	-22 ± 1.85
Art-loaded Niosome	183 ± 6.47	0.827	-13 ± 4.45
Metf/Art-loaded Niosome	207.4 ± 4.21	0.574	-18.4 ± 3.46

and 207.4 ± 4.21 nm, respectively (Fig. 1). The small size of nanoparticles has increased their surface-to-volume ratio, which leads to problems such as aggregation of NPs. An important effective factor in aggregation is the zeta potential of NPs. Table 1 shows the DLS results of the nanoparticles. Recent studies demonstrated that

PEGylated-niosome could enhance the blood circulation, half-life, retention effect, and permeability of the drug to the cell membrane [70]. Nanoparticle morphology plays a significant role in various aspects, including toxicity, dissolution, properties, and performance in different applications. The choice of nanoparticle morphology can impact the interaction of nanoparticles with cellular membranes and the dissolution of the material [71]. The morphology of niosomes can vary depending on the formulation and the specific drug being loaded. Microscopy evaluation of niosomes has shown that they have a multi-layer and spherical morphology [72]. The morphology of fabricated niosomal NPs were surveyed with the FE-SEM (Fig. 2) and AFM (Fig. 3) techniques. The image of ANP-MNP admitted the spherical shape and identical dispersion of the drug.

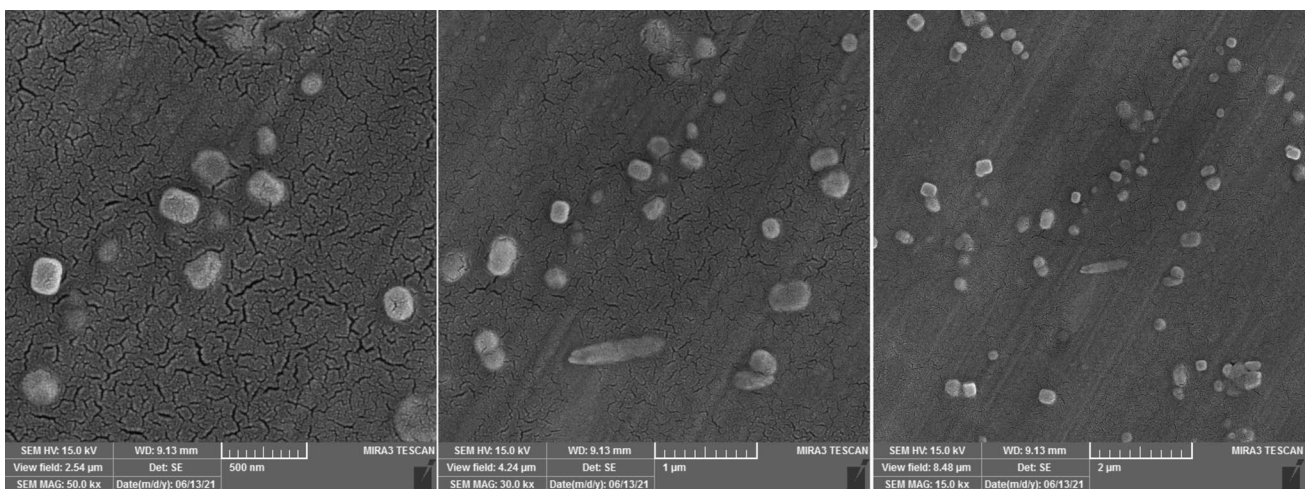


Fig. 2 Characterization of Nio-NPs morphology applying FE-SEM. FE-SEM is a powerful imaging technique that combines the principles of scanning electron microscopy (SEM) with field emission (FE) characteristics

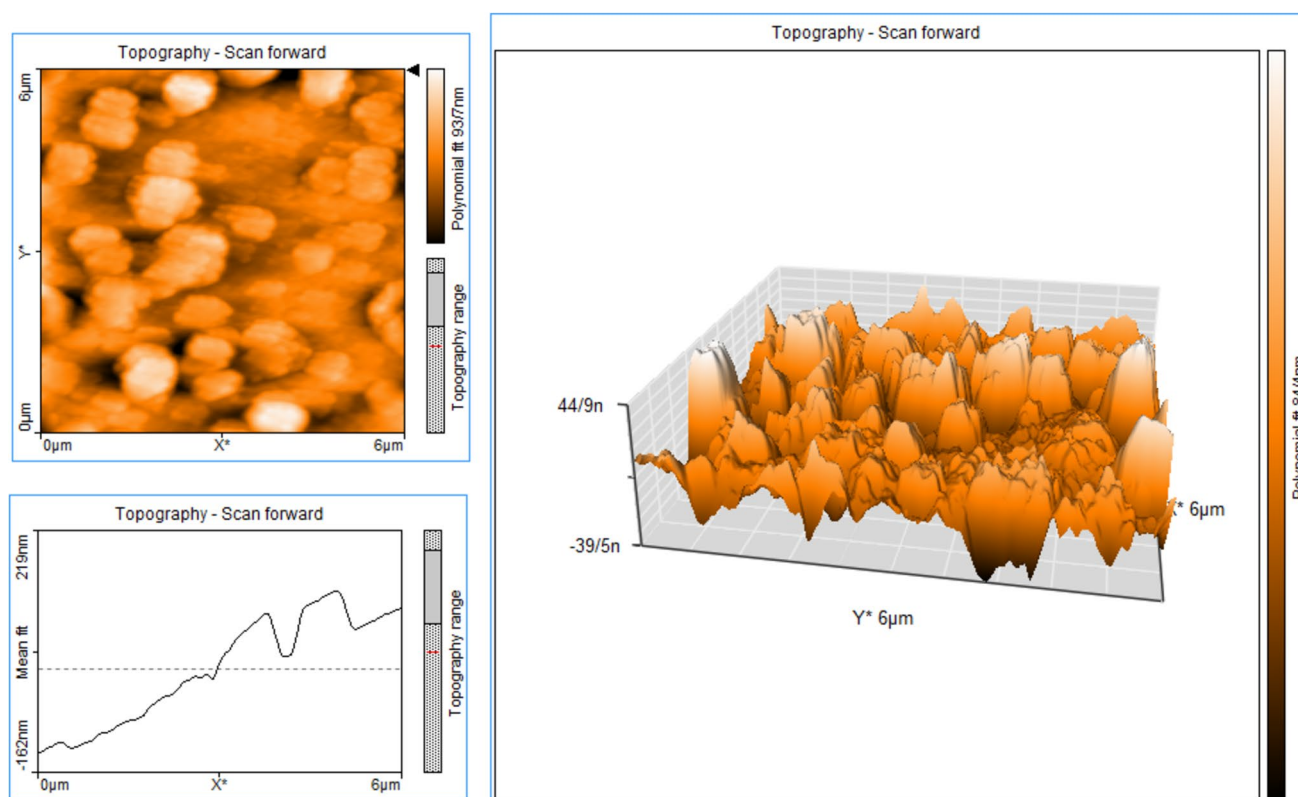


Fig. 3 Characterization of Nio-NPs by AFM technique. AFM operates by scanning a sharp probe tip over the surface of a sample, measuring the forces between the tip and the sample to create a high-resolution image

Characterization by FTIR

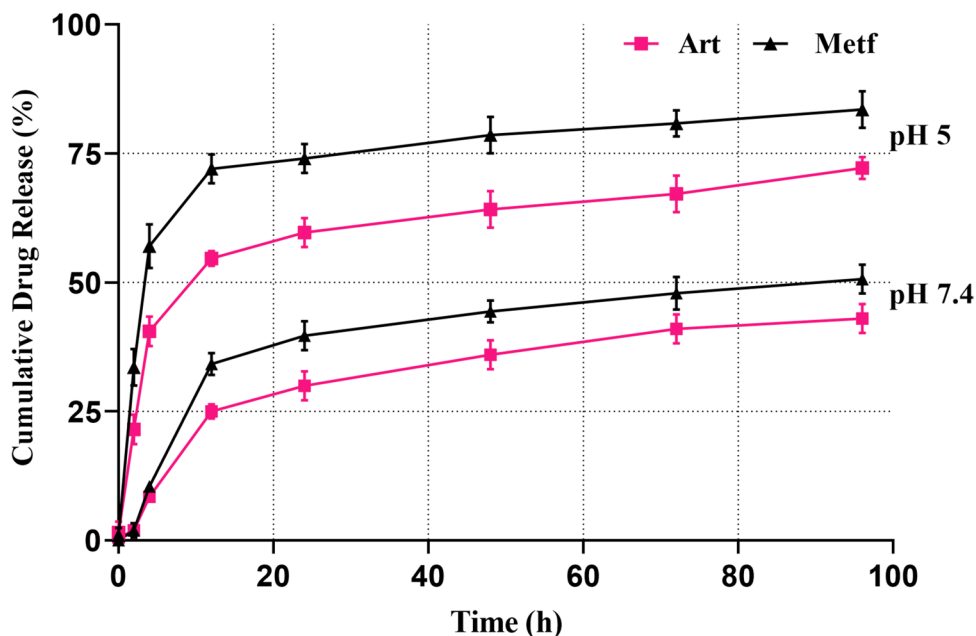
The physicochemical structure of cholesterol, span 60, PEG, ART, MET, blank Nio-NPs, ANP, MNP, and ANP-MNP are shown in Figure S1. The spectrum of span showed peaks at 2893 cm^{-1} and 2836 cm^{-1} (CH stretching, asymmetric and symmetric aliphatic respectively), and 1168 cm^{-1} ($-\text{C}-\text{CO}-\text{O}-$). Cholesterol displayed characteristic peaks of methylene rocking at 789 cm^{-1} , and C–H bond stretching in the range of $2800\text{--}3000\text{ cm}^{-1}$. PEG showed an absorption band at 1637 cm^{-1} (C=C aliphatic double bond), and 1726 cm^{-1} (C=O). The FTIR spectrum of MET demonstrated two typical peaks at 3357 cm^{-1} (N–H asymmetric stretching), and 1651 cm^{-1} (C=N stretching). The FTIR spectra of ART characterized by a peak at 1728 cm^{-1} (C=O stretching vibrations), and 1107 cm^{-1} (–O– stretching vibrations). The remaining synthesis compounds included these mentioned peaks, which indicate the presence of these substances in their ingredients.

Drug release and drug loading efficiency analysis

The loading efficiency of drugs into niosomes can vary depending on the specific drug and the formulation of

the niosomes. For example, a study on diosgenin-loaded niosomes reported a relatively high loading efficiency of approximately 89% [73]. The loading efficiency of hydrophilic drugs may be influenced by the larger aqueous internal volume of niosomes [74]. It has been demonstrated that cholesterol and Span 60 in the niosome structure could increase the amount of the hydrophobic drug loading into them [75]. ANP and MNP both demonstrated biphasic releasing pattern under physiological ($\text{pH}=7.4$) and cancerous ($\text{pH}=5$) conditions (Fig. 4). As previous studies explained the untrapped drugs (ART and MET) which are connected to the surface of Nio-NPs with a weak bond, are released in the first hours of the experiment and result in the sharp slope of the graph [76]. A study by Davarpanah et al., demonstrated that PEGylation of niosomes resulted in a slower release compared to naked niosomes containing the drug by improving the kinetics of drug release from niosomes [77]. The findings demonstrated that the ART and MET were gradually released from ANP and MNP, exhibiting a gentle and slow gradient. Our results support earlier research that affirmed the beneficial impact of niosome on drug release [78]. Both ANP and MNP show a higher amount of release in $\text{pH}=5$ in comparison to $\text{pH}=7.4$, that allows the Nio-NPs to be transported by the blood circulation ($\text{pH}=7.4$) and

Fig. 4 Drug release patterns of ART and MET released from Nio-NPs in PBS solution at pH 7.4 and 5. These results demonstrated a biphasic releasing pattern for niosomes under different pH



release higher amounts of the drugs after reaching the target sites (pH=5) [79]. These findings reveal that ANP and MNP are sensitive to different pH.

In vitro cytotoxicity and synergistic analysis

After 48 h of treatment with various concentrations of agents, MTT analysis was performed to examine the combined cytotoxic effectiveness of ART, MET, ANP, and MNP on A549 lung cancer cells. Recent studies have shown the cytotoxic effects of pure ART and MET on A549 cells, which are in accordance with the results of this study [27,

80]. As illustrated in Fig. 5, Both ANP and MNP effectively suppressed the proliferation of A549 cells in a dose-dependent manner. The IC₅₀ values of drugs are reported in Table 2. As shown in Table 2 the nano-formulation forms of drugs had substantially higher cytotoxicity toward A549 cells after 48 h of treatment, indicating that the prompting mechanism for drug release from the niosome into the cytoplasm was particularly successful. Furthermore, according to the results of the MTT assay, we calculated the synergistic effect of drugs via the median-effect (Compusyn) method. As expected, the combination and niosome conserved form of MET and ART showed additional growth inhibitory

Fig. 5 Cytotoxicity of ART, MET and their nano-form on A549 lung cancer cell viability. Cell viability was measured using MTT assay after 48 h treatment. Data represented are from three independent experiments

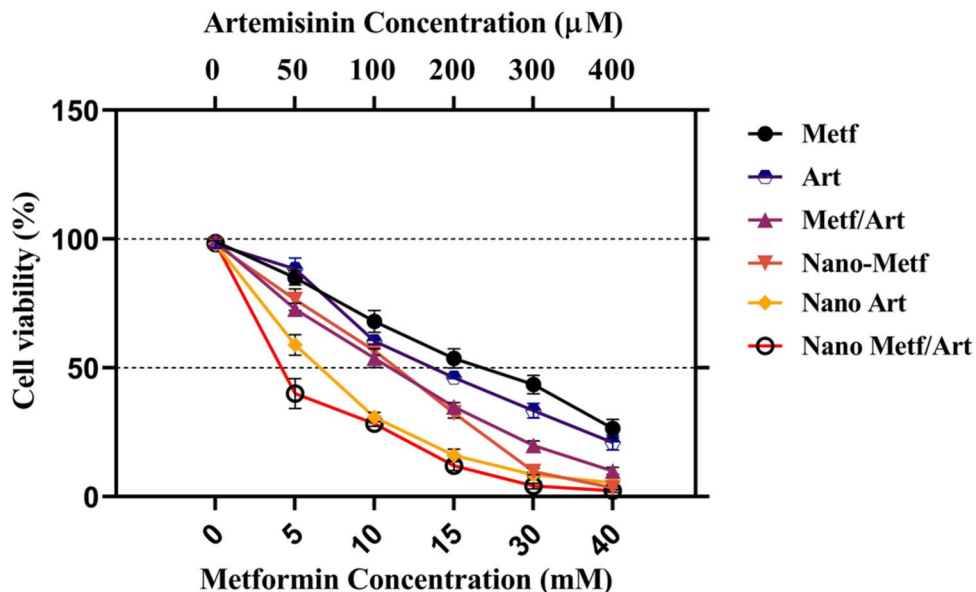


Table 2 IC₅₀ values of drugs evaluated with MTT assay. The MTT test is a widely used method for measuring cell proliferation and cytotoxicity. It involves the reduction of MTT, a tetrazolium salt, by metabolically active cells to formazan products, which can be quantified colorimetrically

Form	Metformin	Artemisinin	Metf in Combination	Art in combination	CI
Pure	14.6 mM	195.2 μM	9.61 mM	98.3 μM	0.643
Nano	78.3 μM	56.7 μM	38.5 μM	31.6 μM	0.475

effect with an extreme drop in IC₅₀ on the lung cancer cells than MET and ART in free and single form after 48 incubation time. The enhanced cytotoxic effects of the ANP and MNP combination might be attributed to greater cellular absorption, extra intracellular concentrations, and effective anticancer agent interactions. These findings are consistent with prior research that showed the anti-proliferative efficacy of MET and ART against several kinds of lung cancer cell lines [19, 27]. Based on these results the IC50 concentration of drugs was used as treatment groups in the rest of the experiments.

Real time PCR

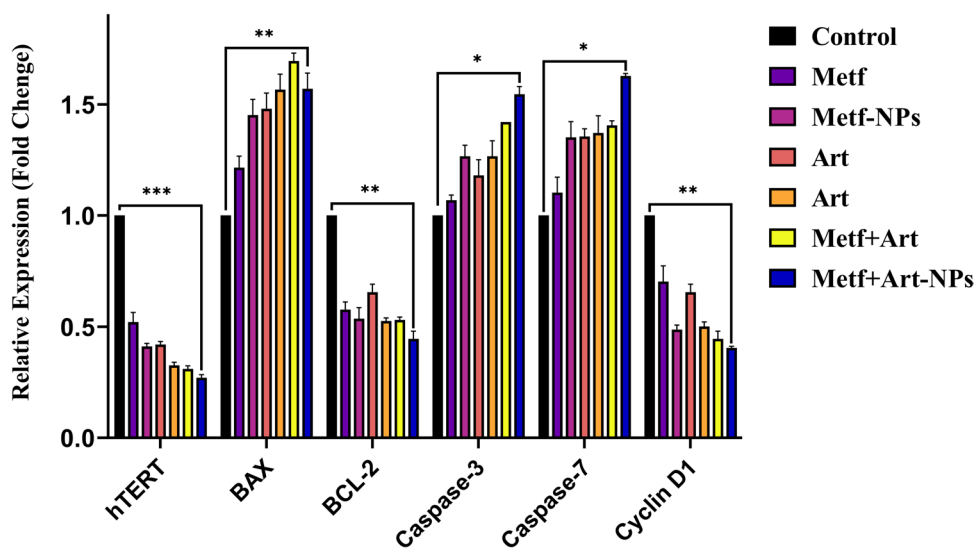
RT-PCR was used to evaluate the effect of ART, MET, MNP, ANP, and their combinations on A549 cells gene expression. The expression levels of hTERT, caspase-3, caspase-7, BAX, BCL-2, and Cyclin D1 genes are reported in Fig. 6. The process of apoptosis and its performance is through various pathways by activating a group of caspase proteins that regulate apoptosis and BCL-2 proteins, which have anti-apoptotic and pro-apoptotic effects. Some studies have shown that high expression of hTERT or its mutations may be connected with migration and metastasis of cancer cells [13]. Statistical analysis showed that 80% of cancers have active telomerase while in healthy cells it is inactive. The results showed that after 48 h of treatment,

ANP, and MNP significantly increased the mRNA level of BAX, caspases 3 and 7 and decreased mRNA levels of BCL-2, hTERT, and Cyclin D1 compared to free form of ART, and MET (Fig. 6). Accordingly, PEGylated Nio-NPs containing drugs are an appropriate approach in the treatment of various cancers, especially lung cancer [58].

Apoptosis analysis

The apoptosis effects of drugs on A549 cells were evaluated with annexin assay and flow cytometry (Fig. 7). Recent studies have proven the apoptotic effect of ART and MET on lung cancer [27, 81], which is consistent with the results of this study. Apoptosis induction analysis also revealed the synergistic effects of ART and MET. Among treated cells, the late apoptosis and early apoptosis of cells treated with a combination of ANP and MNP were highest. As shown in Fig. 7, ANP and MNP combination significantly induced apoptosis of A549 cells more than other forms, furthermore, both ANP and MNP exhibited a greater cytotoxic effect compared to their pure form, which demonstrates the increase in the uptake of ART and MET from Nio-NPs by the cells. These findings are consistent with earlier research, which indicated that the intracellular release of the drugs from NPs is responsible for the cytotoxic effect of NPs [82].

Fig. 6 The expression changes of hTERT, Cyclin D1, BAX, BCL-2, Caspase 3, and 7 genes in A549 cells after 48 h treatment via free and Nano formulated drugs. (p value < 0.001 ***, p value < 0.01 **, p value < 0.05 *)



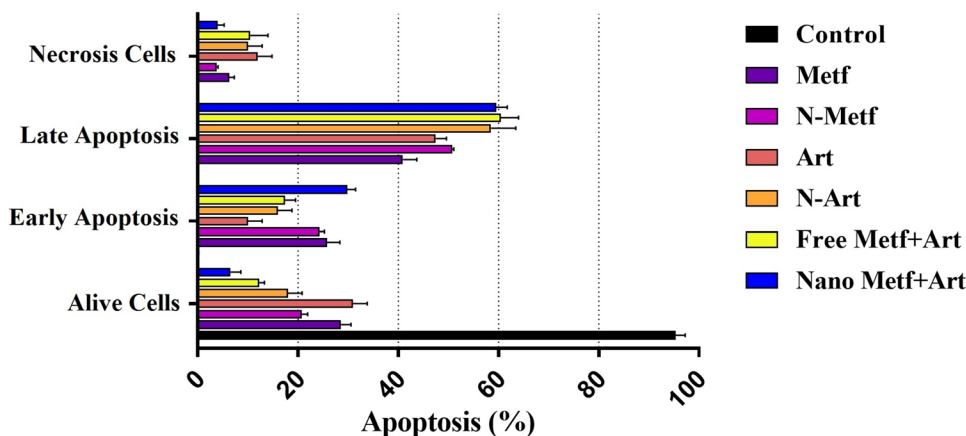


Fig. 7 Identification of apoptosis by the flow cytometric assay of Annexin V/PI staining. The flow cytometric assay utilizes dot plot diagrams to illustrate different cell populations based on Annexin-V FITC and PI staining. In the panels, the lower left quadrants indicate the presence of viable cells, characterized by a negative response to

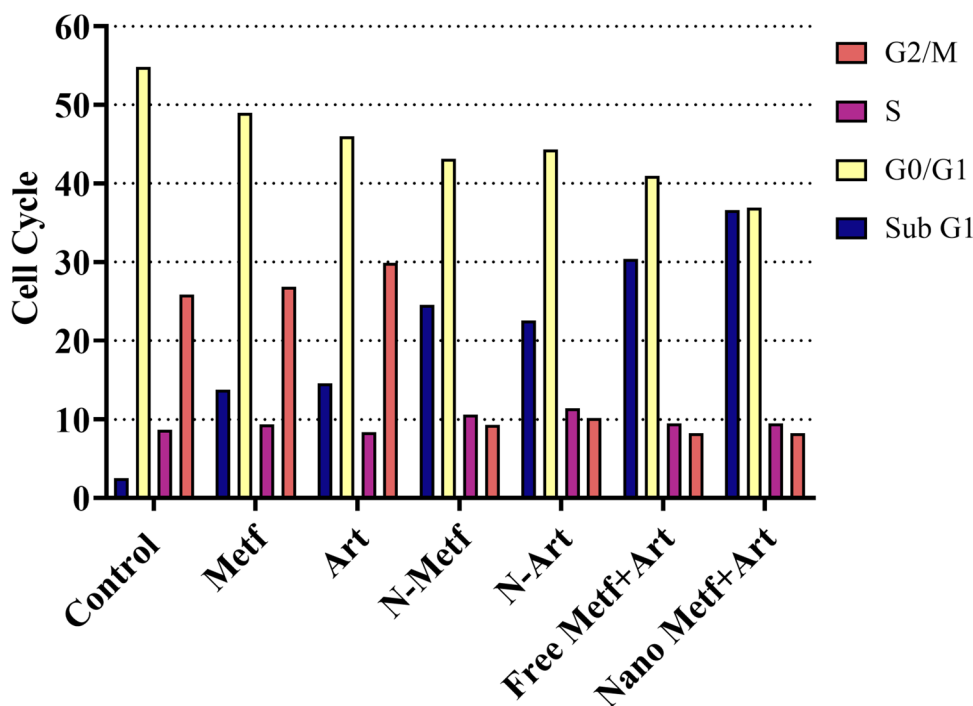
Annexin V and PI staining. The lower right quadrants represent early apoptotic cells, showing positive Annexin V staining but negative PI staining. The upper right quadrants depict late apoptotic cells, displaying positive staining for both Annexin V and PI

Cell cycle analysis

The cell cycle is a highly regulated process that controls the growth and division of cells. It consists of several phases, including G1, S, G2, and M phases. The progression through these phases is tightly regulated by various molecular mechanisms [83]. Several studies have investigated the effects of different agents on the cell cycle. For example, an artemisinin derived agent has induced G1 cell cycle arrest in A549 cells [84]. Cell cycle regulation is not only important

for normal cell growth and development but also plays a critical role in cancer. Dysregulation of the cell cycle is a hallmark of cancer, characterized by uncontrolled proliferation [85]. In the current study, the growth inhibition mechanisms of drugs on A549 lung cancer cells were investigated using cell cycle analyses. Figure 8 shows the control group with normal cell cycle phases (G0/G1, S, G2/M) while another phase can be seen in the treated groups (Sub G1). By changing the drugs from the free form to Nio-NPs loaded form of the same drug, the number of cells in the Sub-G1

Fig. 8 Effect of free and Nano formulated drug on the Cell cycle of A549 lung cancer cells



phase increased, and the highest peaks of the Sub-G1 phase were found in the cells treated by the combination of ANP and MNP.

Conclusion

In the current study, PEGylated Nio-NPs synthesized by the thin-film hydration method were used as nanocarriers for MET and ART against A549 lung cancer cells. Both free MET and free ART showed anticancer activities against lung cancer cells. The effect of MET-ART-loaded NPs was greater than the free form of MET and ART. Moreover, the outcomes of this investigation indicated that when tumor cells were exposed to MET-ART-loaded Nio-NPs, the expression of the hTERT and Cyclin D1 genes were considerably decreased. Also, the most ideal result in the induction of apoptosis and the cell cycle arrest was related to the combined use of MET-ART-loaded Nio-NPs. Although this study investigated a new strategy for treating lung cancer, future studies should be done on the effects of these drugs in vivo experiments.

Supplementary Information The online version contains supplementary material available at <https://doi.org/10.1007/s40199-023-00495-7>.

Funding The authors declare that no funds were received during the preparation of this manuscript.

Availability of data and materials The data and materials that support the findings of this study are available from the corresponding author, upon reasonable request.

Declarations

Ethical approval Not applicable.

Consent to participate Not applicable.

Consent to publication Not applicable.

Conflict of interest No potential competing interest was reported by the authors.

References

- Zhang Y, et al. Global Patterns and Trends in Lung Cancer Incidence: A Population-Based Study. *J Thorac Oncol*. 2021;16(6):933–44.
- Siegel RL, et al. Cancer Statistics, 2021. *CA Cancer J Clin*. 2021;71(1):7–33.
- Oser MG, et al. Transformation from non-small-cell lung cancer to small-cell lung cancer: molecular drivers and cells of origin. *Lancet Oncol*. 2015;16(4):e165–72.
- Zheng M. Classification and Pathology of Lung Cancer. *Surg Oncol Clin N Am*. 2016;25(3):447–68.
- Huang CY, et al. A review on the effects of current chemotherapy drugs and natural agents in treating non-small cell lung cancer. *Biomedicine (Taipei)*. 2017;7(4):23.
- Shafiei G et al. Targeted delivery of silibinin via magnetic niosomal nanoparticles: potential application in treatment of colon cancer cells. *Front Pharmacol*. 2023;14:1174120
- Davoudi Z, et al. Molecular target therapy of AKT and NF- κ B signaling pathways and multidrug resistance by specific cell penetrating inhibitor peptides in HL-60 cells. *Asian Pac J Cancer Prev*. 2014;15(10):4353–8.
- Abdulzehra S, Jafari-Gharabaghloou D, Zarghami N. Targeted delivery of oxaliplatin via folate-decorated niosomal nanoparticles potentiates resistance reversion of colon cancer cells. *Heliyon*. 2023;9(11):e21400
- Olaku O, White JD. Herbal therapy use by cancer patients: a literature review on case reports. *Eur J Cancer*. 2011;47(4):508–14.
- Luo H, et al. Naturally occurring anti-cancer compounds: shining from Chinese herbal medicine. *Chin Med*. 2019;14(1):48.
- Kamarudin MNA, et al. Metformin in colorectal cancer: molecular mechanism, preclinical and clinical aspects. *J Exp Clin Cancer Res*. 2019;38(1):1–23.
- Yang B, Shi J. Developing new cancer nanomedicines by repurposing old drugs. *Angew Chem Int Ed*. 2020;59(49):21829–38.
- Yu H, et al. The Potential Effect of Metformin on Cancer: An Umbrella Review. *Front Endocrinol (Lausanne)*. 2019;10:617.
- Saraei P, et al. The beneficial effects of metformin on cancer prevention and therapy: a comprehensive review of recent advances. *Cancer Manag Res*. 2019;11:3295–313.
- Gupta G, et al. A clinical update on metformin and lung cancer in diabetic patients. *Panminerva Med*. 2018;60(2):70–5.
- Ghorbanzadeh F, et al. Advanced nano-therapeutic delivery of metformin: potential anti-cancer effect against human colon cancer cells through inhibition of GPR75 expression. *Med Oncol*. 2023;40(9):255.
- Jafari-Gharabaghloou D, et al. Potentiation of Folate-Functionalized PLGA-PEG nanoparticles loaded with metformin for the treatment of breast Cancer: possible clinical application. *Mol Biol Rep*. 2023;50(4):3023–33.
- Jafari-Gharabaghloou D, Jabbari A, Soltani A. 187P Development of a magnetic nanostructure for co-delivery of metformin and silibinin on growth of lung cancer cells: possible action through leptin gene and its receptor regulation. *Ann Oncol*. 2022;33:S116.
- Xiao K, et al. The effect of metformin on lung cancer risk and survival in patients with type 2 diabetes mellitus: A meta-analysis. *J Clin Pharm Ther*. 2020;45(4):783–92.
- Mohammadinejad S, Jafari-Gharabaghloou D, Zarghami N. Development of PEGylated PLGA Nanoparticles Co-Loaded with Bioactive Compounds: Potential Anticancer Effect on Breast Cancer Cell Lines. *Asian Pac J Cancer Prev: APJCP*. 2022;23(12):4063.
- Zi F, et al. Metformin and cancer: An existing drug for cancer prevention and therapy. *Oncol Lett*. 2018;15(1):683–90.
- Hassani N, et al. The effect of dual bioactive compounds artemisinin and metformin co-loaded in PLGA-PEG nano-particles on breast cancer cell lines: potential apoptotic and anti-proliferative action. *Appl Biochem Biotechnol*. 2022;194(10):4930–45.
- Konstat-Korzenny E et al. Artemisinin and Its Synthetic Derivatives as a Possible Therapy for Cancer. *Med Sci (Basel)*. 2018;6(1):19
- Li D, Zhang J, Zhao X. Mechanisms and Molecular Targets of Artemisinin in Cancer Treatment. *Cancer Invest*. 2021;39(8):675–84.
- Kiani BH, et al. Artemisinin and its derivatives: a promising cancer therapy. *Mol Biol Rep*. 2020;47(8):6321–36.
- Alibakhshi A, et al. An update on phytochemicals in molecular target therapy of cancer: potential inhibitory effect on telomerase activity. *Curr Med Chem*. 2016;23(22):2380–93.

27. Zhang Q, et al. Artemisinin Derivatives Inhibit Non-small Cell Lung Cancer Cells Through Induction of ROS-dependent Apoptosis/Ferroptosis. *J Cancer*. 2021;12(13):4075–85.
28. Mokhtari RB, et al. Combination therapy in combating cancer. *Oncotarget*. 2017;8(23):38022.
29. Dashti MR, et al. G Protein-Coupled Receptor 75 (GPR75) As a Novel Molecule for Targeted Therapy of Cancer and Metabolic Syndrome. *Asian Pac J Cancer Prev*. 2023;24(5):1817–25.
30. Firouzi-Amandi A, et al. Development, characterization, and in vitro evaluation of cytotoxic activity of Rutin loaded PCL-PEG nanoparticles against Skov3 ovarian cancer cell. *Asian Pac J Cancer Prev: APJCP*. 2022;23(6):1951.
31. Alagheband Y, et al. Design and fabrication of a dual-drug loaded nano-platform for synergistic anticancer and cytotoxicity effects on the expression of leptin in lung cancer treatment. *J Drug Deliv Sci Technol*. 2022;73:103389.
32. Monsen RC, et al. The hTERT core promoter forms three parallel G-quadruplexes. *Nucleic Acids Res*. 2020;48(10):5720–34.
33. Hannen R, Bartsch JW. Essential roles of telomerase reverse transcriptase hTERT in cancer stemness and metastasis. *FEBS Lett*. 2018;592(12):2023–31.
34. Khosravi-Maharlooei M, et al. Expression pattern of alternative splicing variants of human telomerase reverse transcriptase (hTERT) in cancer cell lines was not associated with the origin of the cells. *Int J Mol Cell Med*. 2015;4(2):109.
35. Chen RJ, et al. P53-dependent downregulation of hTERT protein expression and telomerase activity induces senescence in lung cancer cells as a result of pterostilbene treatment. *Cell Death Dis*. 2017;8(8):e2985.
36. Barkhordari A, et al. Potential Anti-Cancer Effect of Helenalin as a Natural Bioactive Compound on the Growth and Telomerase Gene Expression in Breast Cancer Cell Line. *Asian Pac J Cancer Prev: APJCP*. 2023;24(1):133.
37. Suvarna V, Singh V, Murahari M. Current overview on the clinical update of Bcl-2 anti-apoptotic inhibitors for cancer therapy. *Eur J Pharmacol*. 2019;862:172655.
38. Carrington EM, et al. Anti-apoptotic proteins BCL-2, MCL-1 and A1 summate collectively to maintain survival of immune cell populations both in vitro and in vivo. *Cell Death Differ*. 2017;24(5):878–88.
39. Zhou M, et al. Caspase-3 regulates the migration, invasion and metastasis of colon cancer cells. *Int J Cancer*. 2018;143(4):921–30.
40. Walsh JG, et al. Executioner caspase-3 and caspase-7 are functionally distinct proteases. *Proc Natl Acad Sci*. 2008;105(35):12815–9.
41. Lamkanfi M, Kanneganti T-D. Caspase-7: a protease involved in apoptosis and inflammation. *Int J Biochem Cell Biol*. 2010;42(1):21–4.
42. Caglar HO, BirayAvci C. Alterations of cell cycle genes in cancer: unmasking the role of cancer stem cells. *Mol Biol Rep*. 2020;47(4):3065–76.
43. Kaldis P. The cdk-activating kinase (CAK): from yeast to mammals. *Cell Mol Life Sci CMLS*. 1999;55(2):284–96.
44. Amirsaadat S et al. Potential anti-proliferative effect of nano-formulated curcumin through modulating micro RNA-132, Cyclin D1, and hTERT genes expression in breast cancer cell lines. *J Clust Sci*. 2023;8:1–10
45. Kato J-Y, et al. Direct binding of cyclin D to the retinoblastoma gene product (pRb) and pRb phosphorylation by the cyclin D-dependent kinase CDK4. *Genes Dev*. 1993;7(3):331–42.
46. Bonelli M, et al. Multiple effects of CDK4/6 inhibition in cancer: From cell cycle arrest to immunomodulation. *Biochem Pharmacol*. 2019;170:113676.
47. Musgrove EA, et al. Cyclin D as a therapeutic target in cancer. *Nat Rev Cancer*. 2011;11(8):558–72.
48. Wagh VD, Deshmukh OJ. Itraconazole Niosomes Drug Delivery System and Its Antimycotic Activity against *Candida albicans*. *ISRN Pharm*. 2012;2012:653465.
49. Arunachalam A, et al. Niosomes: a novel drug delivery system. *Int J Novel Trends Pharm Sci*. 2012;2(1):25–31.
50. Bhardwaj P et al. Niosomes: A review on niosomal research in the last decade. *J Drug Deliv Sci Technol*. 2020;56:101581
51. Shahbazi R, et al. Design and optimization various formulations of PEGylated niosomal nanoparticles loaded with phytochemical agents: potential anti-cancer effects against human lung cancer cells. *Pharmacol Rep*. 2023;75(2):442–55.
52. Ali Hadi Z, et al. Design and Development of Fe3O4@Prussian Blue Nanocomposite: Potential Application in the Detoxification of Bilirubin. *Asian Pac J Cancer Prev*. 2023;24(8):2809–15.
53. Ge X, et al. Advances of non-ionic surfactant vesicles (niosomes) and their application in drug delivery. *Pharmaceutics*. 2019;11(2):55.
54. Umamaheswari A, et al. Green synthesis of zinc oxide nanoparticles using leaf extracts of *Raphanus sativus* var. *Longipinnatus* and evaluation of their anticancer property in A549 cell lines. *Biotechnol Rep*. 2021;29:e00595.
55. Gurunathan S, et al. Platinum nanoparticles enhance exosome release in human lung epithelial adenocarcinoma cancer cells (A549): oxidative stress and the ceramide pathway are key players. *Int J Nanomed*. 2021;16:515.
56. Amirsaadat S, et al. Metformin and Silibinin co-loaded PLGA-PEG nanoparticles for effective combination therapy against human breast cancer cells. *J Drug Deliv Sci Technol*. 2021;61:102107.
57. Alshetaili AS. Gefitinib loaded PLGA and chitosan coated PLGA nanoparticles with magnified cytotoxicity against A549 lung cancer cell lines. *Saudi J Biol Sci*. 2021;28(9):5065–5073
58. Guo M et al. Cediranib Induces Apoptosis, G1 Phase Cell Cycle Arrest, and Autophagy in Non-Small-Cell Lung Cancer Cell A549 In Vitro. *BioMed Res Int*. 2021:5582648
59. Kis B, et al. Inorganic Element Determination of Romanian Populus nigra L. Buds Extract and In Vitro Antiproliferative and Pro-Apoptotic Evaluation on A549 Human Lung Cancer Cell Line. *Pharmaceutics*. 2021;13(7):986.
60. Firouzi-Amandi A, et al. Chrysin-nanoencapsulated PLGA-PEG for macrophage repolarization: Possible application in tissue regeneration. *Biomed Pharmacother*. 2018;105:773–80.
61. Hawash M, et al. The impact of filtered water-pipe smoke on healthy versus cancer cells and their neurodegenerative role on AMPA receptor. *Drug Chem Toxicol*. 2022;45(5):2292–300.
62. Yoo J, et al. Active targeting strategies using biological ligands for nanoparticle drug delivery systems. *Using*. 2019;11(5):640.
63. Dang Y, Guan J. Nanoparticle-based drug delivery systems for cancer therapy. *Smart Mater Med*. 2020;1:10–9.
64. Rizvi SA, Saleh AM. Applications of nanoparticle systems in drug delivery technology. *Saudi Pharm J*. 2018;26(1):64–70.
65. Momekova DB, Gugleva VE, Petrov PD. Nanoarchitectonics of multifunctional niosomes for advanced drug delivery. *ACS Omega*. 2021;6(49):33265–73.
66. Rasul A et al. In vitro characterization and release studies of combined nonionic surfactant-based vesicles for the prolonged delivery of an immunosuppressant model drug. *Int J Nanomedicine*. 2020;7937–7949.
67. Solomun JI, et al. Manual versus microfluidic-assisted nanoparticle manufacture: impact of silk fibroin stock on nanoparticle characteristics. *ACS Biomater Sci Eng*. 2020;6(5):2796–804.
68. Hajizadeh MR, et al. In vitro cytotoxicity assay of D-limonene niosomes: an efficient nano-carrier for enhancing solubility of plant-extracted agents. *Res Pharm Sci*. 2019;14(5):448.
69. Barani M, et al. Evaluation of carum-loaded niosomes on breast cancer cells: Physicochemical properties, in vitro cytotoxicity, flow cytometric, DNA fragmentation and cell migration assay. *Sci Rep*. 2019;9(1):7139.

70. Minamisakamoto T, et al. Sequential administration of PEG-Span 80 niosome enhances anti-tumor effect of doxorubicin-containing PEG liposome. *Eur J Pharm Biopharm.* 2021;169:20–8.
71. Buchman JT, et al. Understanding nanoparticle toxicity mechanisms to inform redesign strategies to reduce environmental impact. *Acc Chem Res.* 2019;52(6):1632–42.
72. Barani M, et al. In vitro and in vivo anticancer effect of pH-responsive paclitaxel-loaded niosomes. *J Mater Sci - Mater Med.* 2021;32:1–13.
73. Hajizadeh MR, et al. Diosgenin-loaded niosome as an effective phytochemical nanocarrier: Physicochemical characterization, loading efficiency, and cytotoxicity assay. *DARU J Pharm Sci.* 2019;27:329–39.
74. Durak S, et al. Niosomal drug delivery systems for ocular disease—Recent advances and future prospects. *Nanomaterials.* 2020;10(6):1191.
75. Jadon PS, et al. Enhanced oral bioavailability of griseofulvin via niosomes. *AAPS PharmSciTech.* 2009;10:1186–92.
76. Jadid MFS et al. Enhanced anti-cancer effect of curcumin loaded-niosomal nanoparticles in combination with heat-killed *Saccharomyces cerevisiae* against human colon cancer cells. *J Drug Deliv Sci Technol.* 2023;80:104167
77. Davarpanah F, et al. Magnetic delivery of antitumor carboplatin by using PEGylated-Niosomes. *DARU J Pharm Sci.* 2018;26:57–64.
78. Barani M, et al. In silico and in vitro study of magnetic niosomes for gene delivery: The effect of ergosterol and cholesterol. *Mater Sci Eng, C.* 2019;94:234–46.
79. El-Ridy MS, et al. Metformin hydrochloride and wound healing: from nanoformulation to pharmacological evaluation. *J Liposome Res.* 2019;29(4):343–56.
80. Nazim UM, et al. Activation of autophagy flux by metformin downregulates cellular FLICE-like inhibitory protein and enhances TRAIL-induced apoptosis. *Oncotarget.* 2016;7(17):23468.
81. Wu N, et al. Metformin induces apoptosis of lung cancer cells through activating JNK/p38 MAPK pathway and GADD153. *Neoplasma.* 2011;58(6):482–90.
82. Zaki NM. Augmented cytotoxicity of hydroxycamptothecin-loaded nanoparticles in lung and colon cancer cells by chemosensitizing pharmaceutical excipients. *Drug Deliv.* 2014;21(4):265–75.
83. Kamranvar SA, Rani B, Johansson S. Cell cycle regulation by integrin-mediated adhesion. *Cells.* 2022;11(16):2521.
84. Cheong DH, et al. Anti-malarial drug, artemisinin and its derivatives for the treatment of respiratory diseases. *Pharmacol Res.* 2020;158:104901.
85. Prasedya ES, et al. Carrageenan delays cell cycle progression in human cancer cells in vitro demonstrated by FUCCI imaging. *BMC Complement Altern Med.* 2016;16(1):1–9.

Publisher's Note Springer Nature remains neutral with regard to jurisdictional claims in published maps and institutional affiliations.

Springer Nature or its licensor (e.g. a society or other partner) holds exclusive rights to this article under a publishing agreement with the author(s) or other rightsholder(s); author self-archiving of the accepted manuscript version of this article is solely governed by the terms of such publishing agreement and applicable law.